

12-2-2020

Fabrication of High Pours Ti-6Al-4Fe Alloy for Biomedical Application.

Montasser Dewidar

*Materials and Design Department., High Institute of Energy., South Valley University., Aswan., Egypt.,
dewidar5@hotmail.com*

Jae Lim

*Automobile Hi-Technology Research Institute, Chonbuk National University. Duckjin 1-664-14, Jeonju, JB
561-756, South Korea.*

Follow this and additional works at: <https://mej.researchcommons.org/home>

Recommended Citation

Dewidar, Montasser and Lim, Jae (2020) "Fabrication of High Pours Ti-6Al-4Fe Alloy for Biomedical Application.," *Mansoura Engineering Journal*: Vol. 33 : Iss. 1 , Article 9.

Available at: <https://doi.org/10.21608/bfemu.2020.126966>

This Original Study is brought to you for free and open access by Mansoura Engineering Journal. It has been accepted for inclusion in Mansoura Engineering Journal by an authorized editor of Mansoura Engineering Journal. For more information, please contact mej@mans.edu.eg.

Fabrication of high porous Ti-6Al-4Fe alloy for biomedical applicationMontasser M. Dewidar^{1,a}, Jae Kyoo Lim²¹Department of Materials and Design, High Institute of Energy, South Valley University, Aswan, Egypt.²Automobile Hi-Technology Research Institute, Chonbuk National University, Duckjin 1-664-14, Jeonju, JB 561-756, South Korea.^aDewidar5@hotmail.com**عملية تصنيع سبيكة عالية المسامية من التيتانيوم والالومنيوم والحديد بغرض استخدامها في التطبيقات الطبية**

في هذه الدراسة تم استحداث وتطوير سبيكة من التيتانيوم والالومنيوم والحديد وذلك كبدل لسبيكة التيتانيوم والالومنيوم والفاناديوم في صناعة الأجزاء التي تستخدم في الاغراض الطبية كالأجزاء التي تغرس في جسم الكائن الحي بدلا للعظام الطبيعية التي تصاب بالامراض أو تتلف نتسجة الحوادث، وتمتاز هذه السبيكة بتوافقها وتعايشها مع الخلايا الحية عن نظيرتها المصنوعة من التيتانيوم والالومنيوم والفاناديوم لإستبدال الفاناديوم بالحديد حيث اثبتت الأبحاث العلمية أن وجود عنصر الفاناديوم يقلل من العمر الافتراضي للجزء المغروس، وقد تم اعداد هذه السبيكة باستخدام طريقة الطحن الميكانيكي للمساحيق.

وقد تم صناعة عينات بنسبة مسامية 70% عن طريق استخدام طريقة حافظ الفراغات، وقد تم استخدام مسحوق كلوريد الصوديوم (ملح الطعام) ذات حبيبات غير منتظمة الشكل وبحجم يتراوح ما بين 100 و 600 ميكرون كحافظ للفراغات، ثم تم ازالة حافظ الفراغات من العينات عن طريق وضعها في حمام من الماء الساخن عند درجة حرارة 70 درجة مئوية ولمدة خمس ساعات، وقد تمت عملية التليد للعينات في فرن مفرغ الهواء عند درجة حرارة 1250 درجة مئوية ولمدة ساعتين.

وقد اظهرت العينات الملبدة مسام متصلة شبيهة بالموجودة بالعظام الطبيعية، كما تم تعيين الخواص الميكانيكية للعينات وسجل اجهاد الضغط قيمة 38,5 ميجاباسكال كما كانت قيمة معايير المرونة 10,4 جيجاباسكال، ومن النتائج وجد أن الخوص الطبيعية والميكانيكية للعينات تشابه خواص العظام الطبيعية.

Keywords: Titanium-based alloy; Ball milling; Space-holder; Porosity; Mechanical properties

Abstract. In the present study, Ti-6Al-4Fe alloy was developed as a cost effective option to replace the traditional Ti-6Al-4V alloy in the manufacture of surgical implants because of its larger biocompatibility (free vanadium). This alloy was prepared using the ball milling technique. Novel Ti-6Al-4Fe alloy foams with porosity of approximately 70% were fabricated by a space-holder and powder metallurgical process. Irregular NaCl powders with particle size ranging from 100 to 600 μm were used as a space holder material. The NaCl in the green compact was removed in hot distilled water at 70°C for times ranging from 1 to 5 h. The sintering process was performed in a vacuum furnace at 1250°C for 2 h. The Ti-6Al-4Fe alloy foams displayed an interconnected porous structure resembling bone. The compressive stress and the Young's modulus of the Ti-6Al-4Fe foam were 38.5±4 MPa and 10.4±2 GPa, respectively. Both the porous structure and the mechanical properties of the Ti-6Al-4Fe foam were very close to those of natural bone.

Accepted March 31, 2008.

1. Introduction

Human joints are prone to degenerative and inflammatory diseases that result in pain and stiffness of joints [1]. Approximately 90% of the population over the age of 40 suffers from some degree of degenerative joint disease [2]. When natural joints cannot function optimally, they can be replaced by artificial biomaterials. The ideal recipe for a biomaterial to be used for implant application is excellent biocompatibility with no adverse tissue reactions, excellent corrosion resistance in the body fluid, high mechanical strength and fatigue resistance, low modulus, low density, and good wear resistance [3]. Research in this area has received increasing attention. Different artificial implant biomaterials, such as metals, polymeric materials and ceramics are being explored to replace diseased bones. However, the traditional implant biomaterials suffer from problems of adverse reaction, insufficient mechanical properties and lack of ability to induce bone tissue regeneration, shortening the lifetime of the implant biomaterials [4, 5]. Thus, there is an increasing demand to develop new biomaterials in bone tissue engineering, capable of overcoming all or some of these problems. Therefore, development of new alloys is continuously trialed for the following purposes; 1) to remove toxic elements, 2) to decrease the Young's modulus to avoid "stress shield" in bone fixation, 3) to improve tissue and blood compatibility and 4) to miniaturize medical devices.

Pure titanium and some of its alloys, e.g. Ti-6Al-4V, and Ti-29Nb-13Ta-4.6Zr [6, 7] have already found a wide range of applications in implant biomaterials under load-bearing conditions. Ti-6Al-4V alloy demonstrates higher strength and lower elastic modulus than that of pure titanium. The alloy is being used as implant material in high stress-bearing situations, such as hip and knee prostheses, as well as trauma fixation devices for the last two decades. However, since a long time the use of the alloy has been questioned because of black debris containing high levels of titanium, vanadium and aluminum that are found in surrounding tissue under conditions of high

wear, such as in knee and hip implants [8]. While no toxic effects have been linked to this black debris, safety concerns about the vanadium and aluminum have been raised in literature [9]. Piazza et al. [8] reported that aluminum is poorly absorbed within the gastrointestinal tract. Very little amount gets into the blood stream, and hence it appears nontoxic. Yu et al. [10] reported that vanadium can alter the kinetics of the enzyme activity associated with cells of the inflammatory response. Vanadium contained in this alloy has been associated with potential cytotoxic effects and adverse tissue reactions [8].

The titanium-based alloy with aluminum and iron appears to be more suitable for implant applications. It is thus presumable that, Ti-Al-Fe alloy has a high biomedical potential due to its unique property combinations of biocompatibility, bioactivity and mechanical properties. The Ti-5Al-2.5Fe alloy possesses similar corrosion resistance and mechanical properties to those of the Ti-6Al-4V alloy [11]. More importantly, the iron-containing alloy has no apparent toxicity. The surgical implant alloys are used for a long time (20 years). Therefore, the hydrolysis of different compounds of the passive film is possible. The toxicity of dissolved metal ions may cause pain and restrict action in the tissues adjoining the implants. In order to avoid such situation, the wear and corrosion resistance of bioimplants needs to be high. Therefore it is crucial to develop new Ti based alloy parts with high strength.

In this study, a new biocompatible alloy Ti-6Al-4Fe was prepared by ball milling process. High porous Ti-6Al-4Fe samples were fabricated via a space-holder and powder metallurgical process. The space holder method allows a direct near net-shape fabrication of foamed implant components having an elastic modulus comparable to that of natural bone and with a relatively homogeneous pore structure and a high level of porosity. The characteristics of the Ti-6Al-4Fe alloy powder and porous parts were characterized and evaluated using x-ray diffraction pattern (XRD) and scanning electron microscopy (SEM). The mechanical properties

of porous parts were examined by compressive testing.

2. Experimental Procedures

Starting materials were pure elemental powders of titanium, aluminum and iron with reagent purity (99.8 %). The particle size is less than 40 μm for titanium powder 35 μm for aluminium powder and 0.5 μm for iron. The Ti, Al, and Fe powders were weighed to yield the predetermined stoichiometric composition of Ti-6Al-4Fe and mixed together thoroughly. All powders were milled in a tumbling ball mill. The ball-to-powder weight ratio was controlled at 20:1 and powder to alcohol weight ratio of about 2:1 and 25 g of powders were loaded for each run. The elemental powder mixtures were sealed into a polyethylene bottle using zirconia ball at a horizontal rotation velocity of 250 rpm for 48 h. The milling conditions were the same for all batches. After milling, the slurries were dried at 70°C in a vacuum drying oven for 24 h. The process of fabrication porous Ti-6Al-4Fe alloy parts consisted of six main steps as preparing starting metal powders, ball milling, mixing the alloy powder with space-holding particles, compacting, water leaching, and sintering as shown in Figure 1. At first, elemental titanium powder, aluminium powder and iron powder were milled into Ti-6Al-4Fe alloy powder.

The particle size of NaCl ranged from 100 to 600 μm , which was carefully sieved to ensure that the finishing Ti-6Al-4Fe parts exhibiting a porous structure with this pore size distribution. The weight ratios of the Ti-6Al-4Fe powder to the amount of space holder (NaCl) were calculated to obtain defined theoretical porosities of 70% in the sintered compact specimens.

The actual density of compact green specimens before removing the space holder was determined from the weight and size of the compacted specimens while the theoretical density (ρ_{th}) is estimated using the following equation:

$$\rho_{th} = \frac{\rho_{NaCl} \times V_{NaCl} + \rho_{Ti} \times V_{Ti}}{(V_{NaCl} + V_{Ti})} \quad (1)$$

where ρ_{NaCl} and V_{NaCl} are the density and volume of the NaCl respectively, and ρ_{Ti} and V_{Ti} are the density and the volume of Ti-6Al-4Fe powder. From this equation, it can be seen that the theoretical density of the mixture (green specimen) depends on the percentage of space holder and Ti-6Al-4V powder percentage into the specimen i.e. porosity. The estimated theoretical density of specimen with porosity 70% is equal to 2.8655 g/cm³.

The Ti-6Al-4Fe powders were mixed thoroughly with carbamide particles in a rolling container for an hour. To prevent the powder from segregation a small amount of ethanol was sprinkled during titanium powder/ carbamide particles blending. The titanium powder particles adhered to the surface of the space holder. All the specimens used in the present investigation were fabricated by cold compaction using a controlled operated uniaxial press. The mixture was uniaxially pressed at 390MPa into cylindrical compacts with diameter $d=12$ mm. The height of the cylindrical specimens after pressing was approximately 15 mm. The mixing of any additional lubricant is not necessary. This is of special importance for the manufacturing of Ti-4Al-6V parts, where lubricant could be an additional source of impurities in the final product.

The density was calculated by divided the mass of the compact by its volume, which was calculated from physical dimensions. The NaCl in the green compact was removed in hot distilled water at 70°C for times ranging from 1 to 5 h. Specimens were removed from the water bath at regular intervals, dried in air at 70 °C for 5 h and weighted in order to determine the amount of NaCl removed. A vacuum furnace was used for the sintering. The sintering process was performed at 1250°C for 2 h.

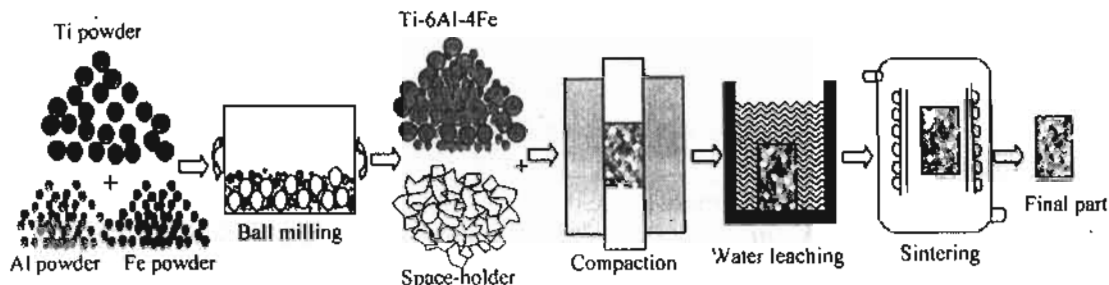


Figure 1. Schematic illustration of the fabrication process for porous Ti-6Al-4Fe

X-ray diffraction patterns and scanning electron microscopy (SEM) were used to characterize the Ti-6Al-4Fe alloy porous samples. A compression test was carried out on the Ti-6Al-4Fe porous sample at room temperature with an initial strain rate of 0.5 mm/s to examine the mechanical properties.

3. Results and discussion

The effect of leaching time on the water leaching behavior of NaCl at 70°C is shown in Figure 2. As verified in the figure, the NaCl removal rate decreased with leaching time, representing that the initial removal rate was higher since the water was in direct contact with the NaCl. The removal rate decreased as leaching time increased due to the increased length of porous channels through which the NaCl must pass through to diffuse out. It should be pointed out that 100% removal is obtained within 4 h. A homogenous macropore distribution was attained throughout the green compact during the water leaching stage. The pore shape replicated the initial shape of the NaCl powder particles that were used to produce the green compact. In addition, the NaCl was completely removed by this process without distortion or slumping of the compacts. After NaCl removal, the strength of the green compacts was sufficient for handling.

The X-ray diffraction patterns for the ball milled powders, and after heat sintering at 1250 °C for 2 h are shown in Figure 3. It can be found that the mixture of powder after milling consists mainly of α Ti, Al_3Fe , and, α Al which proves that the Al_3Fe can be in situ synthesized by ball milling (see Figure 3a). After sintering α -Ti and TiFe are detected, however, small amount of the β -Ti phase is detected in XRD pattern (Figure 3b). In addition, the absent of any phase of Na or Cl means that the NaCl was removed entirely after dissolution in hot water. The apparent density is calculated as the weight of a sample over the volume. The porosity is one minus the relative density. Microstructures of samples with different porosity and pore size are characterized by SEM and shown in Figure 4. Figure 5 is the EDS spectra of Figure 4. It is seen that there are only three kinds of peaks which correspond to titanium, aluminum, and iron respectively. Based on the EDS spectra and XRD we can identify that there is no remaining for NaCl in final part.

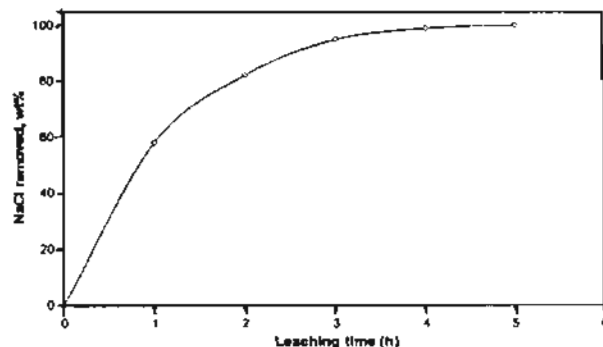


Figure 2. The effect of leaching time on the water leaching behavior of NaCl at 70°C

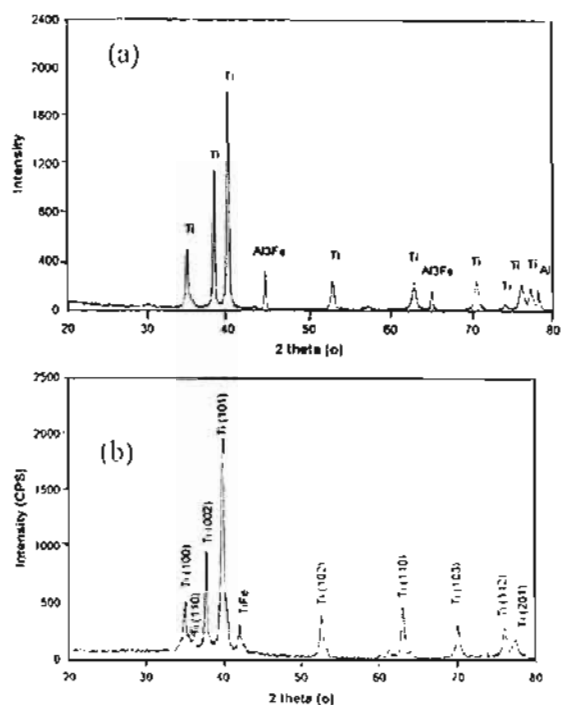


Figure 3. XRD patterns of Ti-6Al-4Fe after a) ball milling, and b) sintering at 1250°C for 2h.

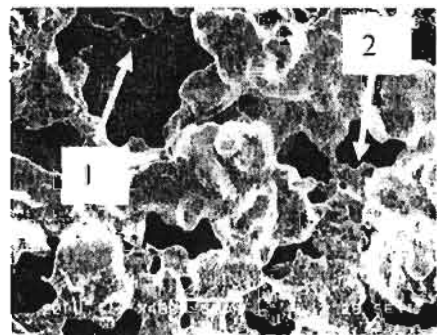


Figure 4. Picture of microstructures of some pores of "1" macropores and "2" micropores.

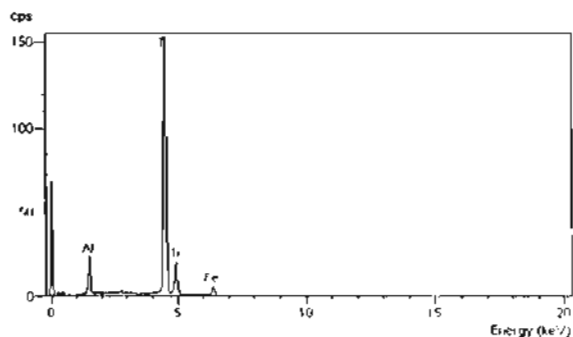


Figure 5 EDS spectra of elements Ti, Al and Fe

Figure 6 shows the SEM of the Ti-6Al-4Fe foam sample with porosity 70%. Microstructural observations revealed that the Ti-6Al-4Fe foam sample exhibited a bimodal porous structure, i.e. macropores and micropores. The macropores of the Ti-6Al-4Fe alloy foam were interconnected throughout the whole sample and their sizes lay between 100–600 μm . The pore size for the macropores was specifically tailored for the ingrowth of the new bone tissues. In addition, the Ti-6Al-4Fe foam displayed another type of pores, i.e. micropores (see Figure 6 b). The micropores had a size of only several microns. Such kind of bimodal porous structure is expected to permit the ingrowth of new bone tissues and vascularization.

Chemical compositions of the particles were analyzed by EPMA, as listed in Table 1. This table present the chemical compositions of two points which indicated in Figure 6 a, and b. The composition for Point 1 is close to the matrix Ti-6Al-4Fe. The Point 1 is considered to be the real composition of the alloy because the detected area is large. On the other hand, the chemical composition of Point 2, which close to the boundary of the particles shows a high concentration of Al and Fe. This means that the fine particles of Al and Fe were covered the particles of Ti.

To evaluate the mechanical properties, compressive test was conducted on Ti-6Al-4Fe alloy foam with a porosity of 70%. Figure 7 shows the stress–strain curve for the Ti-6Al-4Fe foam sample. It can be seen that the Ti-6Al-4Fe foam showed the typical deformation behavior of metallic foams under compressive loading. The stress–strain curve can be divided into three regions, that is, an elastic deformation region at the beginning of deformation, a plateau region with a nearly constant stress to a large strain, and a densification region where the stress increases rapidly. The compressive plateau stress and the Young's modulus of the Ti-6Al-4Fe foam were 38.5 ± 4 MPa and 10.4 ± 2 GPa, respectively.

At low strain level, the stress of the specimen with pores parallel to the compressive direction is higher than that of specimen with pores

perpendicular. However, this tendency is reversed with increasing strain. While the stress concentration occurs around the pores in the specimen with pores perpendicular to the compressive direction, there is little stress concentration around the pores in the specimen with the cylindrical pore parallel to the compressive direction. The stress concentration is important factor for determination on the strength of porous metals. The pores perpendicular to the compressive direction are easily deformed at lower stress. It can be explained that the pores in the perpendicular case is easily crushed during compression due to the stress concentration around the pores. Consequently, such anisotropy of the slope of the stress-strain curves may be attributed to the stress concentration and the volume fraction of pores.

In practical applications, porous scaffold design needs to consider both the strength and the Young's modulus to achieve a functionally satisfying implant. The compressive strength of bone ranges from 2 to 200 MPa and the elastic modulus ranges from 10 to 40 GPa [12]. To avoid stress shielding, which may lead to bone resorption and even necrosis, the elastic moduli of bone and implants should be as similar as possible. It can be seen that the mechanical properties of the Ti-6Al-4Fe foam were very close to those of the natural bone. Depending on some factors such as the type, age, gender, and race it should be noted that the mechanical properties of natural bones are different. So, the requirements of the mechanical properties for the implant materials change accordingly. Further research is needed to cope with the detailed requirements for each implant material to match those of the specific bone.

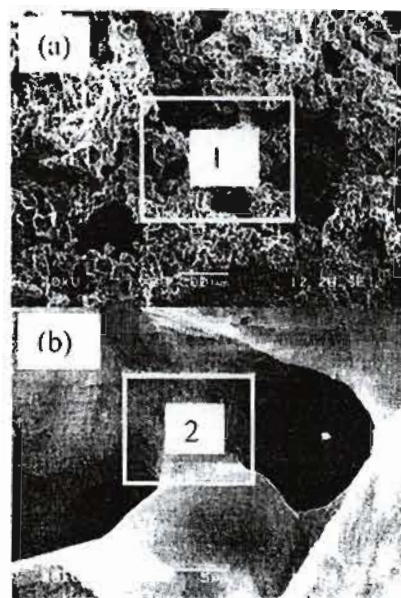


Figure 6. a) macropores of Ti-6Al-4Fe foams, and b) micropores

Table 2 EPMA analysis results of particles formed in the titanium alloy matrix

Element	Point 1		Point 2	
	wt %	at. %	wt %	at. %
Al	3.62	6.26	7.68	12.96
Fe	2.08	1.74	5.66	4.62
Ti	94.30	91.99	86.66	82.42

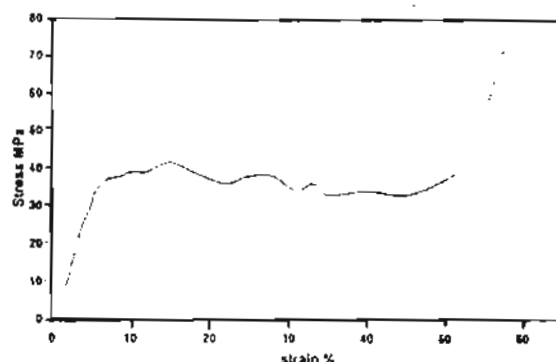


Figure 7. Stress - strain of a Ti-6Al-4Fe alloy foam with porosity 70% under compressive loading.

3. Conclusions

Ti-6Al-4Fe foams with macropores and micropores structure were fabricated by using

powder that was prepared by ball milling and space holder technique. A water leaching and sintering process was successfully developed for manufacturing Ti-6Al-4Fe samples with a porosity of 70%. In this process, NaCl was used as a space holder and was completely removed from the green samples by water leaching at 70°C without distortion of the samples. The green samples had sufficient strength for handling after water leaching. This process is capable of producing net-shape Ti-6Al-4Fe samples with controlled pore morphology, size, distribution and porosity. The pore size of the macropores in the foams ranged between 100–600 μm , which was tailored for new bone tissue ingrowth. There were also micropores distributed on the macropore-edges with a size of several microns, which is expected to be beneficial to vascularization. The compressive stress and the Young's modulus of the Ti-6Al-4Fe foam were 38.5 ± 4 MPa and 10.4 ± 2 GPa, respectively. Both the porous structure and the mechanical properties of the foam were very close to those of natural bone. Further work will be done to investigate the biocompatibility of this alloy.

Acknowledgment

The research reported in this paper was supported by the Korea Research Foundation (KRF). The authors would like to thank the KRF for their support.

References

- [1] M. Long, and H. J. Rack *Biomaterials* 19, 1621-1639, 1998
- [2] S. Nag, R. Banerjee, J. Stechschulte, and H. L. Fraser, Comparison of microstructural evolution in Ti-Mo-Zr-Fe and Ti-15Mo biocompatible alloys," *Journal of Materials Science: Materials In Medicine* 16 (2005) 679–685
- [3] H. J. Rack, and J. I. Qazi, "Titanium alloys for biomedical applications," *Materials Science and Engineering C* 26 (2006) 1269 – 1277
- [4] J. R. Woodard, A. J. Hildore, S. K. Lan, C.J. Park, A. W. Morgan, J.C. Eurell, and G.C. Sherrie *Biomaterials*, 28, 1, 2007, 45-54.
- [5] D.W. Hutmacher, *Biomaterials* 21 (2000) 2529.
- [6] T. Kasuga, M. Nonami, M. Niinomi, and T. Hattori, *Biomaterials* 24 (2003) 238.
- [7] Y. Okazaki, *Biomaterials* 23 (2002) 2071.
- [8] S. Piazza, G. Lo Biundo, M.C. Romano, C. Sunseri, and F. Di Quarto, *Corros. Sci.* 40 (1998) 1087.
- [9] K. Wang, *Mater. Sci. Eng. A* 213 (1996) 134.
- [10] J. Yu, Z. J. Zhao, and L.X. Li, *Corros. Sci.* 35 (1993) 587.
- [11] E. Leitão, R. A. Silva and M. A. Barbosa *Corrosion Science*, 39, (1997), 377.
- [12] M. Dewidar, H-C Yoon, and J.K. Lim, *Metals and Materials*, 12, 3, (2006), 193.